NIH Public Access
Author Manuscript
Respir Physiol Neurobiol. Author manuscript; available in PMC 2009 February 1.

Published in final edited form as:
Respir Physiol Neurobiol. 2008 February 1; 160(2): 147–159.

Hypercapnia modulates synaptic interaction of cultured brainstem neurons

Liang Yang, **Junda Su**, **Xiaoli Zhang**, and **Chun Jiang**
Department of Biology, Georgia State University, 33 Gilmer St., Atlanta, GA 30303

Summary

CO_2 is an important metabolic product whose concentrations are constantly monitored by CO_2 chemoreceptors. However, the high systemic CO_2 sensitivity may not be achieved by the CO_2 chemoreceptors without neuronal network processes. To show modulation of network properties during hypercapnia, we studied brainstem neurons dissociated from embryonic rats (P17–19) in multi-electrode arrays (MEA) after initial period (3 weeks) of culture. Spike trains of 33,622 pairs of units were analyzed using peri-event histograms (PEH). The amplitude of pericentral peaks between two CO_2-stimulated units increased and the peak latency decreased during hypercapnia. Similar enhancement of synaptic strength was observed in those sharing a common input. These phenomena were not seen in CO_2-unresponsive neurons. The amplitude of pericentral peaks between two CO_2 inhibited units also increased without changing latency. Over 60% CO_2-stimulated neurons studied received mono-/oligosynaptic inputs from other CO_2-stimulated cells, whereas only ~10% CO_2-unresponsive neurons had such synaptic inputs. A small number of brainstem neurons showed electrical couplings. The coupling efficiency of CO_2-stimulated but not CO_2-unresponsive units was suppressed by ~50% with high PCO_2. Inhibitory synaptic projections were also found, which was barely affected by hypercapnia. Consistent with the strengthening of excitatory synaptic connections, CO_2 sensitivity of post-synaptic neurons was significantly higher than presynaptic neurons. The difference was eliminated with blockade of presynaptic input. Based on these indirect assessments of synaptic interaction, our PEH analysis suggests that hypercapnia appears to modulate excitatory synaptic transmissions, especially those between CO_2-stimulated neurons.

Keywords

CO_2 chemoreceptor; multielectrode arrays; MEA; peri-event histogram; cross-correlation; cell culture; neuronal network; electrical coupling

1, Introduction

CO_2 is a major metabolic product and plays an important role in systemic pH regulation and acid-base secretions. The PCO_2 levels are tightly regulated by several feedback control systems in which a critical step is the CO_2 detection by sensing cells in the brainstem and carotid body (Feldman et al. 2003; Richerson 2004; Putnam et al. 2004; Guyenet et al. 2005b). Of particular interest are brainstem CO_2-chemosensitive neurons, as the systemic CO_2 response is retained after carotid bodies are removed bilaterally. With these CO_2-chemosensitive cells, the nervous system can detect a change in arterial PCO_2 by as low as 1 torr and couple it to a 20–30%

* *Correspondence to:* Phone: 404-651-0913, Fax: 404-651-2509, E-mail: cjiang@gsu.edu.

Publisher's Disclaimer: This is a PDF file of an unedited manuscript that has been accepted for publication. As a service to our customers we are providing this early version of the manuscript. The manuscript will undergo copyediting, typesetting, and review of the resulting proof before it is published in its final citable form. Please note that during the production process errors may be discovered which could affect the content, and all legal disclaimers that apply to the journal pertain.

NIH-PA Author Manuscript
NIH-PA Author Manuscript
NIH-PA Author Manuscript

NIH-PA Author Manuscript

NIH-PA Author Manuscript

NIH-PA Author Manuscript

change in ventilation (Feldman et al. 2003; Putnam et al. 2004). Such a systemic response does not seem to be solely medicated by CO_2-sensiting molecules as none of the putative CO_2/pH sensing molecules identified as yet is capable of producing significant alterations in membrane potentials or other cellular activities in response to a change in 1 torr PCO_2 (Jiang et al. 2005). It is possible that the brainstem neuronal networks play a role.

Several groups of CO_2-chemosensitive neurons have been identified in the brainstem, such as serotonergic neurons in midline raphé nuclei, glutamatergic neurons in the retrotrapezoid nucleus, and catecholaminergic neurons in the locus coeruleus (Pineda and Aghajanian 1997; Oyamada et al. 1998; Wang et al. 1998; Filosa and Putnam 2003; Severson et al. 2003; Mulkey et al. 2004). These neurons, that do not belong to any major brainstem respiratory neuronal groups, project to respiratory nuclei modulating postsynaptic neurons (Nattie 1999; Richerson 2004; Putnam et al. 2004). Thus, they are presynaptic with respect to respiratory premotoneurons and motoneurons. Since the latter neurons are also CO_2 chemosensitive (Onimaru et al. 1989; Kawai et al. 1996; Talley et al. 2000; Okada et al. 2002; Guyenet et al. 2005a; Kawai et al. 2006), there may be synaptic interactions between the pre- and postsynaptic neurons allowing the necessary CO_2 signal amplification. Indeed, our recent studies have shown that both pre- and postsynaptic neurons contribute to the CO_2 chemosensitivity of cultured brainstem neurons (Su et al. 2007). Clearly, the understanding of brainstem neuronal CO_2 chemoreception requires the information of not only the intrinsic membrane properties but also the modulation of synaptic interactions during hypercapnia. To show electrophysiology evidence for the modulation of synaptic transmissions by high CO_2, we performed these studies on primary neuronal culture in multi-electrode array (MEA) dishes. Multiple neurons were simultaneously recorded, and their synaptic interactions were examined using peri-event histograms (PEHs), a method that allows an indirect assessment of synaptic transmission.

2. Materials and methods

2,1. Cell culture in microelectrode arrays (MEA) dishes

The MEA dishes were purchased from MCS (Reutlingen, Germany). Each dish has 64 microelectrodes placed in the center (1.5 mm^2) of the glass bottom with inter-electrode space of 200μm. The electrodes are embedded in glass with the tip (30μm in diameter) exposed to the culture medium. There is a larger internal reference electrode for grounding. The dishes can be re-used after cleaning and autoclave. Before culture, 100μl polyethyleneimine (PEI) solution (0.05%) in 0.1 M borate buffer (pH 8.4~8.6) was dropped to the electrode region and kept for 1 hour, followed by plating the area with a 10μl droplet of 0.002% laminin (Sigma, St. Louis, MO) for at least 30 min (Potter and DeMarse 2001; Su and Jiang 2006; Su et al. 2007).

Primary neuronal cultures were prepared from embryonic (days 17–19) rat brainstem, as we described previously (Su and Jiang 2006). In brief, timed-pregnant Sprague Dawley rats were euthanatized by the inhalation of lethal dose halothane (Halocarbon Laboratories, River Edge, NJ), according to the protocols approved by the Institutional Animal Care and Use Committee or IACUC of the Georgia State University. Embryos were removed from the uterus and chilled on ice. All tissues from the lower brainstem containing the whole medulla and pons were micro-dissected into tissue blocks (0.5–1 mm^3) under sterile condition. From each fetus, 4–5 brainstem tissue pieces in ~0.5 mm thickness were obtained. Then each piece was split into two. The tissue blocks from all fetuses in one litter were mixed together and digested in 5 ml papain solution (Worthington-Biochem, Lakewood, N.J.) for 30 min in an incubator with 5% CO_2, 95% air at 37°C. The digested tissues were triturated by using a P-1000 Pipetman. Passing through a 40 μm Falcon filter (BD Biosciences, Bedford, Mass.), the solution was centrifuged at 300 g for 5 min. After discontinuous density gradient centrifuge with albumin-inhibitor

NIH-PA Author Manuscript

NIH-PA Author Manuscript

NIH-PA Author Manuscript

solution at 70 g for 6 min, the cell pellet was immediately re-suspended in culture medium. Dissociated cells (20,000 to 50,000) were plated in a 20 μl droplet covering the 1.5 mm electrode region of an MEA, forming a dense monolayer (Wagenaar et al. 2005). With this protocol, each pregnant animal can be used for 8–10 MEA dishes. To reduce the variability among MEA dishes, great efforts were made to keep the cell mixture as homogeneous as possible, and recordings were performed under the same experimental conditions (Su and Jiang, 2006, Su et al., 2007). However, there was certain variability among MEA dishes, and some dishes showed more responsive neurons than others. The MEA dishes were kept in an incubator (Model NU-4750, Nuaire, Plymouth, MN) with 5% CO_2 and 95% air at 36°C for 20~30 min and then filled with 1.2 ml of the Neurobasal medium (NBM) supplemented with B-27 and GlutaMax-I (GIBCO/Invitrogen, Carlsbad, CA). After 48 hours the NBM was switched to Dulbecco's modified Eagle's medium (DMEM, Irvine Scientific, Santa Ana, CA) with 10% equine serum added (Hyclone, Logan, UT). One half or 2/3 of the medium was replaced with fresh medium twice per week. The dish was covered by a Teflon lid and tightly sealed by a thin membrane of fluorinated ethylene-propylene (Teflon FEP film, 12.5 μm thickness, American Durafilm, Holliston, MA). The film is permeable to CO_2 / O_2, but not to microbes and water vapor (Potter and DeMarse 2001), allowing instant equilibrium of the gas in the MEA culture chamber. Cells were maintained in a constant condition of 36°C, 5% CO_2, and 95% air in the cell culture incubator.

2.2. MEA recording

Extracellular recordings were carried out at 36°C in DMEM by using a preamplifier (MCS MEA1060-2, Reutlingen, Germany), which held one MEA dish and was kept in the incubator during recording. Action potentials were digitized at 40 kHz by using a 64-channel A–D converter with the MEA Workstation software (Plexon Inc., Dallas, TX). Single unit activity was then identified using the OfflineSorter software (Plexon) based on Principal Component Analysis methods (Horn & Friedman, 2003). CO_2 exposure was performed in the tissue culture incubator in which step switch of CO_2 levels was reached within 1 min by the built-in CO_2 sensor and CO_2 controller. At baseline, the chamber was ventilated with 5% CO_2 (PCO_2 38 mmHg). During exposure, the gas was switched to different PCO_2 levels from 20 to 80 mmHg. Recordings were taken in 10 min each. Once the firing frequency of baseline recording was stabilized for consecutive three recordings (30 min) with 5% CO_2 (38 mmHg), step-elevated PCO_2 administration was performed subsequently, followed by three to six washout recordings (30–60 min) with 5% CO_2. Pharmacological blockers were added to the dish with final concentrations calculated according to the volume of culture medium. 10 μM 6-cyano-7-nitroquinoxaline-2,3-dione (CNQX) was used to block glutamatergic AMPA/kainate receptor, and 2mM EGTA/1.4mM Mg^{2+} to block nonspecifically neural transmission. The method to apply halothane (2mM) for the study of electrical coupling was the same as described previously (He and Burt 2000). Chemicals were purchased from Sigma Chemicals (St. Louis, MO).

2.3. Data analysis

Single unit was identified using the OfflineSorter software (Plexon Inc.) based on the Principal Component Analysis methods (Horn and Friedman 2003). The CO_2 sensitive index was calculated by obtaining the response slope value first: slope = $(n\sum xy-(\sum x)(\sum y) / (n\sum x^2-(\sum x)^2)$, where x = PCO_2 (torr), y = spike count. Then, Sensitivity Index C = slope / Max Y, where Max Y is the maximum spike count from among 4 different CO_2 concentrations.

The PEHs were constructed with the Neuroexplorer software (Nex Technologies, Littleton, MA) using spike trains from each unit. Each spike was counted once at the time when it crossed the threshold set in the MEA Workstation software (Plexon Inc.). The spike data were binned in 0.3 or 0.4 ms. Neuronal pairs were randomly made with one of them as reference. Each unit

NIH-PA Author Manuscript

NIH-PA Author Manuscript

NIH-PA Author Manuscript

was paired only once either as reference or target, and no units were paired to themselves. Each spike of the reference was used to average spike trains of the target unit in 40 ms before and after the reference spike. The peak and trough were accepted if they were greater than the confidence level ($P < 0.001$). Units with total spike number less than 200 in a 10 min recording (or 0.3 Hz) were rejected from data analysis. Peaks located at −0.4 ms < 0.4 ms were considered as central peaks. Other peaks and troughs ranging from −6.0 ms to 6.0 ms were considered to be pericentral. The peak width at half magnitude was examined. Units with the peak width > 0.5 ms and < 10 ms were further investigated, which were accepted only when they were found not to be caused by single bin PEH spikes or high frequency oscillation in the neuronal pair. Troughs ranging from 0.5 ms to 10 ms with trough/mean ratio < 0.5 were analyzed. For the electrical coupling, the coupling efficiency was calculated using the peak count in the PEH divided by reference spike number.

Data are presented as means ± S.D. (standard deviation). Differences of CO_2 effects on neuronal activity were examined using ANOVA or paired Student t test. The non-parametric data for cell type distributions were examined with χ^2 test. Differences were considered to be statistically significant if $P \leq 0.05$.

Results

3.1. Primary brainstem culture in MEAs

The cultured neurons started developing processes one day in culture and firing action potentials in 2–3 days. Their firing activity varied in the first 2–3 weeks, became stable after 3 weeks of culture, and remained stable for at least 2 months (Su and Jiang 2006; Su et al. 2007). Thus all recordings were performed within 3–9 weeks of culture.

Neuronal CO_2 chemosensitivity was studied in a tissue culture incubator in which step changes in CO_2 levels is achieved within 1 min. Since firing activity reached plateau in 7–8 min (Su et al. 2007), we chose a 10-min CO_2 exposure in this study. Such a CO_2 exposure augmented firing activity of a group of neurons (Fig. $1A_1$). To quantify CO_2 sensitivity of the brainstem neurons, we measured firing rate (FR) in each unit and plotted it against PCO_2 levels (Fig. 1B). Since the FR of most units showed linear response in the PCO_2 range of 20 to 80 torr, a sensitivity index C was calculated by fitting the response curve with a linear equation (Fig. 1B, see Methods for details), and used to screen single units. A unit was considered to be CO_2-stimulated if $C \geq 0.0067$ (corresponding to a 20% change in FR with a 30 torr change in PCO_2), to be CO_2-inhibited if $C \leq -0.0067$, and to be CO_2-unresponsive otherwise (Su et al. 2007). The CO_2 responses were reversible and reproducible in repetitive exposures (Fig. 1B). Systematical analysis of synaptic interactions was performed after CO_2 response pattern was identified in each unit.

3.2. Changes in excitatory synaptic interaction during hypercapnia

To reveal electrophysiological synaptic interaction, the PEH was constructed for each pair of units with spike trains in a stretch of 10 min recording. Single unit recordings were identified using spike sorting and interspike histograms (Fig. $1A_2$–A_4). Because we were interested in mono- or oligosynaptic connections, our data analysis was focused only on pericentral peaks with latency <6 ms and a half-peak duration < 10ms (see Discussion). Of 33,622 pairs of units studied from total about 50 fetuses in 5 pregnant rats, 472 pairs displayed PEH peaks wider than 0.4 ms and taller than the 99.9% confidence level. Of these 472 peaks, 323 were pericentral peaks, and 149 were central peaks. To assess how the synaptic transmission of these neurons is affected by hypercapnia, we analyzed 1) the ratio of peak versus background firing activity or the peak-mean ratio, 2) peak width, and 3) latency of pericentral peaks.

NIH-PA Author Manuscript

NIH-PA Author Manuscript

NIH-PA Author Manuscript

Of the 33,622 pairs of units, 9,857 pairs had both units to be stimulated by hypercapnia (PCO_2 70 torr). In these units, 62 pairs showed pericentral peaks in the PEHs (Fig. 2A,B). The peak-mean ratio of these CO_2-stimulated units changed from 6.9±8.8 at baseline (PCO_2 38 torr) to 9.8±12.6 during hypercapnia (PCO_2 70 torr, Fig. 2C), corresponding to a 42% increase (P=0.0001, n=61; paired Student t Test). In comparison, no significant difference in the peak-mean ratio was found in the CO_2-unresponsive group (Fig. 2F). The peak latency, an indirect measure of synaptic transmission efficiency and axon conduction velocity, was also affected in these CO_2-stimulated neuronal units, decreasing from 1.9±1.9 ms to 1.5±1.3 ms with the hypercapnia (P=0.01, n=61; Fig. 2D). Such a change was not observed in CO_2-unresponsive units (P=0.61, n=167; Fig. 2G). The peak width measured at 50% peak amplitude remained unchanged during hypercapnia in both groups of units (P=0.31, n=167; Fig. 2E, H).

We also studied 1,636 pairs of units that were both inhibited during hypercapnia (PCO_2 70 torr). In these units, 93 pairs showed pericentral peaks in PEHs (Table 1). The peak-mean ratio of these CO_2-inhibited units changed from 7.9±13.7 at baseline (PCO_2 38 torr) to 9.8±13.1 during hypercapnia (Fig. 2I), corresponding to a 42% increase (P=0.0007, n=92). The latency of CO_2-inhibited units did not show evident reduction during hypercapnia. (P=0.19, n=92; Fig. 2J). The peak width did not change significantly during hypercapnia (P=0.18, n=92; Fig. 2K).

Central peaks were also found in a number of neuronal pairs, suggesting that these cells share a common input (Fig. 3A). Statistic analysis showed that the peak-mean ratio of the central peaks increased significantly in the CO_2-stimulated neurons during high CO_2 exposure, changing from 3.8±2.2 to 4.4±2.7 (P=0.003, n=43) (Fig. 3B, C). The peak duration became significantly wider in the CO_2-stimulated units during hypercapnia (Table 1, Fig. 3D). In contrast, no significant changes in the peak-mean ratio and the peak duration of the central peaks were found in CO_2-unresponsive units (P=0.29, n=52; Fig 3E, F).

A total of 34 central peaks were found in CO_2-inhibited units. Statistical analysis showed that the peak-mean ratio was significantly enhanced during high CO_2 exposure, changing from 9.5 ±13.8 to 11.4±17.1 (P=0.02, n=33) (Fig. 3G). The peak duration in the CO_2-inhibited units did not change during hypercapnia (Fig. 3H, Table 1).

3.3. Modulation in electrical couplings

Some of the central peaks (n=18 pairs) were extraordinary. They fired action potentials almost always simultaneously showing very large peak amplitude in the PEH (Fig. $4A_1$). It is very unlikely that these action potentials were recorded from the same cell, as the two electrodes were separated by at least 200 μm, and the spike distribution was not completely symmetric in the PEH (Fig. $4A_2$). These units did not seem to be recorded from axons either, as the spikes showed typical morphology of somata action potentials (Fig. $4C_1$, D_1) (Gustafsson and Jankowska 1976;Jiang and Lipski 1990). When they were plotted in coupling efficiency against peak-mean ratio, these large central peaks were clearly segregated from the common inputs and pericentral peaks shown above (Fig 5), suggesting that these action potentials were recorded from two neurons with electrical synapses or gap junctions as have been previously observed in brainstem neurons (Huang et al. 1997;Solomon and Dean 2002;Dean et al. 2002). Consistently, the coupling efficiency, i.e., peak spike counts of the target unit divided by spiked counts of the reference unit, was almost completely suppressed in the presence of 2 mM halothane, a gap junction blocker (Fig. 6). Such electrical couplings were observed in CO_2-stimulated (n=5) and CO_2-unresponsive (n=13) units. The coupling efficiency between CO_2-stimulated neurons was significantly reduced during high CO_2 exposure (P=0.006, n=4; Fig. 4B, E), while no significant changes were seen in the CO_2-unresponsive group (P=0.21, n=12; Fig. 4F).

NIH-PA Author Manuscript

NIH-PA Author Manuscript

NIH-PA Author Manuscript

3.4. Inhibitory synaptic connections

Inhibitory synaptic connections shown as PEH troughs were observed in a small number of neurons (Fig. 7A). Of total 6 toughs in 33,622 pairs of units, all reference units were CO_2-stimulated (n=6). The target units were CO_2-unresponsive (n=5) and CO_2-inhibited (n=1). Although the trough width at half trough amplitude increased significantly during high CO_2 exposure (P=0.03, n=5), the latency and trough/mean ratio did not show any significant changes (Fig. 7C–E, Table 1).

3.5. Connection preference of cultured brainstem neurons

With the indirect assessment of PEHs, we studied connection preference of various types of units. Of 122 CO_2-stimulated units, 106 (87%) projected to another CO_2-stimulated units, and only 16 (13%) made synapses with CO_2-unresponsive neurons (Fig. $8A_1$). In comparison, 59 of 205 (29%) CO_2-unresponsive units projected to CO_2-stimulated units, while most of them (146 or 71%) synapsed with CO_2-unresponsive units (Fig. $8A_2$). When looking at the postsynaptic cells (i.e., the receiver unit in the PEH), we found that 106 of 165 (64%) CO_2-stimulated units received mono-/oligosynaptic input from another CO_2-stimulated units, whereas 16 of 162 (10%) CO_2-unresponsive units had such synaptic input (Fig. $8B_1$, B_2). The $\chi 2$ test showed significant difference in the connection preference of the CO_2-stimulated versus CO_2-unresponsive units ($\chi 2=103.3$, $P<0.0001$). CO_2-inhibited neurons also showed a connection preferential. Most of them (93 of 171, 54%) projected to another CO_2 inhibited units, and 78 (46%) project to the CO_2-unresponsive units (Fig $8C_1$). In contrast, 50 of 196 (26%) CO_2-unresponsive units projected to CO_2-inhibited units, while most (146 or 74%) projected to the CO_2-unresponsive units (Fig $8C_2$). When looking at the postsynaptic cells, we found that 93 of 143 (65%) CO_2-inhibited units received mono-/oligosynaptic input from another CO_2-inhibited units, whereas only 78 of 224 (35%) CO_2-unresponsive units had such synaptic input (Fig. $8D_1$, D_2). The $\chi 2$ test showed significant difference in their connection preference ($\chi 2=32.1$, $P<0.0001$).

The CO_2-stimulated units also showed a special distribution in bursting neurons. Of 150 units whose firing patterns could be clearly distinguished, 81 were CO_2-stimulated, and 69 did not show evident response to hypercapnia. Sixty six percent of the CO_2-stimulated units displayed bursting pattern in their firing activity. In contrast, only 23% of the CO_2-unresponsive units showed bursting activity. The distributions were examined with the $\chi 2$ test and showed significant difference ($\chi 2=22.9$, $P<0.0001$).

3.6. Enhancement of CO_2 chemosensitivity

If both pre- and postsynaptic neurons (the driver unit and receiver unit in the PEH, respectively) are stimulated by high PCO_2, they together may enhance the overall CO_2 chemosensitivity of the postsynaptic cells. To test this possibility, we looked at the FR response to hypercapnia. Our results showed that the C value of postsynaptic neurons was significantly higher than that of the presynaptic cells (Fig. 9A). We then blocked synaptic transmission to examine whether some of the CO_2 responses of postsynaptic neurons were derived from presynaptic neurons. Blockade of excitatory synaptic transmission with CNQX (10 μM) resulted in a significant decreases in the C value in the postsynaptic neurons. In the condition of losing some of the presynaptic contributions, the CO_2 sensitivity of postsynaptic neurons became comparable to the presynaptic (Fig. 9B). We also found a group of units that lost CO_2 chemosensitivity almost completely in the presence of 10 μM CNQX (Fig. 9C). Similarly the total elimination of the CO_2 chemosensitivity in such neurons was observed when synaptic transmission was non-specifically blocked with low Ca^{2+} (<1 μM) and high concentrations of Mg^{2+} (2 mM) (Fig. 9D), suggesting that some CO_2-unresponsive postsynaptic cells can gain their CO_2 chemosensitivity from presynaptic neurons.

NIH-PA Author Manuscript

NIH-PA Author Manuscript

NIH-PA Author Manuscript

Changes in the CO_2 chemosensitivity was also examined in the units showing electrical couplings. By random pairing, we did not see any significant difference in the C value (P=0.45, n=4; Fig. 9E). Meanwhile, we noticed that one unit in each pair tend to have lower CO_2 sensitivity than the other. When those with lower C value were pooled together, we found that their C value was significantly lower than their partners (P=0.0004, n=4; Fig. 9F), indicating that these pairs are not equally CO_2-chemosensitive. Since the coupling efficiency decreased in these units (Fig. 4B), our results suggest that the inhibition of these electrical couplings during hypercapnia may confine the CO_2 chemosensitivity to one cell preventing its cellular responses from spreading to another cell.

4. Discussion

Using the MEA technique together with PEH analysis, we have studied CO_2 chemosensitivity of cultured neurons obtained from the lower brainstem where all critical components for central breathing activity are located including neurons for rhythm genesis, respiratory reflexes and CO_2 chemoreception (Feldman et al. 2003). Consistent with previous reports (Neubauer et al. 1991; Rigatto et al. 1994; Wang et al. 1998; Su and Jiang 2006), our results have shown that brainstem neurons in primary culture retain the capability of forming neuronal networks. Such neuronal networks not only are morphological entities but also display clear functional activity. Based on indirect assessments of synaptic transmission with PEHs, several types of synaptic connections indeed have been observed in the present study.

Because of several technical difficulties, we could not obtain neurons from well-defined brainstem nuclei for our primary culture: First, these nuclei are too small and too transparent to identify in the brainstem of fetus rats. Second, the successful neuronal culture relies on a critical mass of the cell numbers. We failed to retain the cultured neurons from a small region around locus coeruleus, even though multiple fetuses were used. We believe that these technical limitations can be overcome with our continuing pursuing and the efforts by other research groups including identification of specific neuronal marks and development of transgenic mice with GFP in certain brainstem nuclei.

Since several brainstem areas necessary for respiratory controls and CO_2 chemosensitivity are included in our cell cultures, some of the dissociated neurons may rejoin each other in culture with synaptic connections, allowing processes of CO_2 chemosensitivity not only by their intrinsic membrane properties but also by neuronal networks. Indeed, our results have shown that neuronal network properties are also targeted by hypercapnic modulation. We believe that this finding is important. Firstly, although theoretically possible, the CO_2 modulation of brainstem neuronal network properties has not been well demonstrated previously, likely owing to technical limitations such as long-term recordings from multiple cells with the conventional electrophysiological approaches. Secondly, although studies on membrane intrinsic properties over the past 6–7 years have led to demonstration of a number of potential molecular sensors for CO_2 detection, the sensitivity of these molecules does not seem adequate for the systemic response to a minute change in PCO_2 levels (Jiang et al. 2005). The involvement of synaptic interaction can lead to amplifications of the CO_2 signal and may satisfy the systemic need in response to hypercapnia. Furthermore, a large number of cells have been shown to be CO_2 chemosensitive (Richerson 2004; Putnam et al. 2004; Jiang et al. 2005), while the biological significance for having so many chemosensitive cells is still unclear. The requirement of pre- and postsynaptic neurons for achieving high CO_2 chemosensitivity provides a potential explanation.

The PEH used in our studies is an effective method for analysis of neuronal network properties. The method is based on the time relationship of spike trains of two neurons. A large of number of studies have proven that neuronal synaptic connections can be well determined by the

NIH-PA Author Manuscript

NIH-PA Author Manuscript

NIH-PA Author Manuscript

method (Kirkwood, 1979; Gerstein 2000; Buzsaki 2004). It was first proposed by Perkel et al. in 1967 with various generations of PEHs or cross-correlations developed later for studies of time domains (Gerstein and Perkel 1972; Gerstein and Aertsen 1985; Palm et al. 1988; Aertsen et al. 1989) and frequency domains (Perkel 1970; Rosenberg et al. 1989). Using the PEH analysis, we observed 472 sharp peaks and 6 troughs in 33,622 pairs of units. The positive connection rate is lower than that among respiratory-modulated units (345 out of 6,471 units, Li et al. 1999), likely due to the presence of neurons in heterogeneous neuronal networks in our cell culture. With these units, we analyzed changes in synaptic strength before and during hypercapnia using the PEH. Synaptic connections were determine using parameters: latency < 6ms, half-peak width < 10ms, which were chosen based on the fact that cultured neurons do not have myelination in their axons (Dugandzijanovakovic and Shrager 1995; Kawaguchi and Fukunishi 1998). Concerning the longest distance in the MEA matrix (2 mm) and the conduction velocity of a typical unmyelinated axon (~0.4 m/s), the transduction of an action potential in the distance with a single synaptic delay (0.5 ms) can be as long as 6 ms, suggesting that most of our pericentral peaks and troughs are monosynaptic. Our results have shown that the latency of pericentral peaks is significantly reduced during hypercapnia in CO_2-stimulated neurons. The reduction in the peak latency can be produced by several presynaptic mechanisms such as a quicker release of neurotransmitters, more vesicles dunked to the synaptic cleft with each action potential and faster conduction velocity in the axon of the presynaptic cell. All the PEH evidence suggests that synaptic transmission is enhanced during hypercapnia. Supporting this idea are our results showing the peak-mean ratio of pericentral and central peaks also increase significantly with high PCO_2. The higher peak-mean ratio is likely to be a result of selective enhancement of synaptic communications between the neuronal pair under the PEH study over other cells that also synapse with these neurons. The higher peak-mean ratio also can be produced by 1) more neurotransmitter release following each action potential in presynaptic neurons, and/or 2) augmentation of postsynaptic receptors by hypercapnia (Chen et al. 2001; Mao et al. 2002; Wemmie et al. 2002). Clearly, the clarification of these issues requires direct measurements of synaptic transmission. Nevertheless, our PEH analysis provide indirect evidence suggesting that synaptic strength of a number of units especially those stimulated by CO_2 is enhanced during high PCO_2. The enhanced synaptic strength appears to contribute to the amplification of CO_2 signals detected by the CO_2-stimulated neurons.

Another interesting finding from our studies is that the CO_2-stimulated neurons tend to make synaptic connections with another CO_2-stimulated cells based on the indirect assessments with PEHs. We have found that over 60% CO_2-stimulated neurons receive mono- or oilgosynaptic presynaptic input from another CO_2-stimulated cells. In contrast, only 10% CO_2-unresponsive units receive such synaptic input. Previous studies have shown that serotonergic neurons in the midline raphé nuclei (Wang et al. 1998; Severson et al. 2003), glutamatergic neurons in the retrotrapezoid nucleus (Mulkey et al. 2004; Guyenet et al. 2005a) and catecholaminergic neurons in locus coeruleus (Pineda and Aghajanian 1997; Oyamada et al. 1998; Filosa and Putnam 2003) are all CO_2 chemosensitive. A general characteristic of these CO_2-chemosensitive cells is that they have extensive synaptic connections with respiratory and non-respiratory neurons in the brainstem. These cells are known to be intrinsically CO_2 chemosensitive, as their CO_2 chemosensitivity is retained after blockade of the synaptic transmission (Oyamada et al. 1998; Wang et al. 1998; Filosa and Putnam 2003; Severson et al. 2003; Mulkey et al. 2004). Since certain respiratory neurons postsynaptic to these cells are also intrinsically CO_2 chemosensitive (Kawai et al. 1996), our finding of selective connections among the CO_2-stimulated neurons in the cultured neuronal networks supports these previous studies. Such a preferential connection among CO_2-stimulated neurons may underscore the necessary neuronal networks for the enhancement of CO_2 chemosensitivity by neurotransmission.

NIH-PA Author Manuscript

NIH-PA Author Manuscript

NIH-PA Author Manuscript

Electrical couplings have been previously shown in brainstem neurons from neonatal rats (Huang et al. 1997; Solomon and Dean 2002; Dean et al. 2002), which is supported by our current studies in cultured brainstem neurons. There are several connexin proteins including connexins 26, 32 and 36 expressed in brainstem neurons, they form gap junction between neurons and coupled electrical and chemical activity between cells (Condorelli et al. 2000; Solomon et al. 2001; Solomon 2003). In the present study, we have observed a group of central peaks that are distinct from the common input for two reasons: 1) their coupling efficiency is extremely high, allowing both cells to fire simultaneously, while such a high coupling efficiency cannot be achieved with chemical synapses as action potentials are usually generated with multiple (>100) unitary PSPs (Kirkwood, 1979); 2) these central peaks are highly sensitive to halothane, a blocker of gap junctions (He and Burt 2000). There are two types of electrical couplings in our cultured brainstem neurons with one inhibited by and the other unresponsive to supporting the existence of multiple connexin proteins in the brainstem (Young and Peracchia 2004). The gap junction channels made of acid-inhibited connexins appear to play a role, as the inhibition of the electrical couplings may limit the CO_2 signal to individual cells leading to diminishing or even blocking the CO_2 response from coupling to other cells.

We also observed a few cells with inhibitory monosynaptic connections. All the presynaptic input comes from CO_2-stimulated neurons. The inhibitory synaptic interaction is only modestly affected by hypercapnia with ~15% increase in the half-trough width. Neither the trough/mean ratio nor trough latency changes with high PCO_2. Since the presynaptic neurons are CO_2-stimulated and increase their firing activity with CO_2 exposure, the lack of effects suggests that postsynaptic (or receptor) responses to neurotransmitters may be reduced during hypercapnia. It is also possible that the CO_2-stimulated presynaptic neurons are different from those synapses with other CO_2-stimulated postsynaptic neurons, which may release neurotransmitters disproportional to action potential frequency. This observation, however, should not exclude the possibility that the inhibitory synaptic connections contribute to CO_2 chemosensitivity of brainstem neurons, as the CO_2-inhibted neurons were not systematically investigated in the present study.

Our results suggest that the modulation of neuronal network properties can lead to an enhancement of the CO_2 chemosensitivity of brainstem neurons. By quantitative comparison of the CO_2 chemosensitivity, we have found that the postsynaptic neurons have significantly higher CO_2 sensitivity than presynaptic neurons. Such a difference is at least partially derived from presynaptic input as it disappears when presynaptic input is blocked (Su et al. 2007). Also, disruption of synaptic transmission with either non-specific blockade or by blocking excitatory glutamatergic input causes a general reduction in the CO_2 chemosensitivity of most neurons. Such an action is more effective in some neurons that lose their CO_2 chemosensitivity completely. Therefore, the presynaptic drives not only can enhance the postsynaptic CO_2 chemosensitivity, but also can enable it in some cells. With the modulation of network properties and synaptic transmission, the CO_2 signal detected by individual cells thus can be shared by other neurons in the networks, and more importantly, the CO_2 signal can be amplified when the postsynaptic cells are also capable of detecting CO_2 with their inherent membrane properties.

It is noteworthy that these observations were made in dissociated brainstem neurons in culture. In our previous studies, we have found that firing activity of the brainstem neurons is stabilized after three weeks of culture which may reflect maturation, and shown evidence for the presence of serotonergic, glutamatergic and catecholaminergic neurons in the culture (Su and Jiang, 2006; Su et al. 2007). Despite these, the connections between these neurons have not been demonstrated to resemble those seen in-vivo. Therefore, the results from the present study need to be validated in other preparations, and the neuronal identities need to be further characterized. Nevertheless, the cultured neurons in MEAs provide an access to central CO_2

NIH-PA Author Manuscript

NIH-PA Author Manuscript

NIH-PA Author Manuscript

chemosensitivity beyond individual neurons, and allow us to appreciate several novel findings on the changes neuronal network properties with hypercapnia.

In conclusion, the network properties of cultured brainstem neurons have been studied in the MEA system. Our results from these studies suggest that the network properties appear to be targeted by hypercapnic modulation. It is likely that the hypercapnic modulation of both network and inherent membrane properties leads to enhancement of synaptic strength and amplification of CO_2 signals detected by brainstem neurons.

Acknowledgments

This work was supported by an NIH grant (HL067890).

Reference List

Aertsen AM, Gerstein GL, Habib MK, Palm G. Dynamics of neuronal firing correlation: modulation of "effective connectivity". J Neurophysiol 1989;61:917.

Bou-Flores C, Berger AJ. Gap junctions and inhibitory synapses modulate inspiratory motoneuron synchronization. J Neurophysiol 2001;85:1543–1551. [PubMed: 11287478]

Buzsaki G. Large-scale recording of neuronal ensembles. Nat.Neurosci 2004;7:446–451. [PubMed: 15114356]

Chen G, Dunbar RL, Gao W, Ebner TJ. Role of calcium, glutamate neurotransmission, and nitric oxide in spreading acidification and depression in the cerebellar cortex. J Neurosci 2001;21:9877–9887. [PubMed: 11739595]

Christie JM, Bark C, Hormuzdi SG, Helbig I, Monyer H, Westbrook GL. Connexin36 mediates spike synchrony in olfactory bulb glomeruli. Neuron 2005;46:761–772. [PubMed: 15924862]

Condorelli DF, Belluardo N, Trovato-Salinaro A, Mudo G. Expression of Cx36 in mammalian neurons. Brain Res Brain Res Rev 2000;32:72–85. [PubMed: 10751658]

Dean JB, Kinkade EA, Putnam RW. Cell-cell coupling in CO(2)/H($^{+}$)-excited neurons in brainstem slices. Respir.Physiol 2001;129:83–100. [PubMed: 11738648]

Dean JB, Ballantyne D, Cardone DL, Erlichman JS, Solomon IC. Role of gap junctions in CO_2 chemoreception and respiratory control. Am J Physiol Lung Cell Mol Physiol 2002;283:L665–L670. [PubMed: 12225940]

Dekin MS, Richerson GB, Getting PA. Thyrotropin-releasing hormone induces rhythmic bursting in neurons of the nucleus tractus solitarius. science 1985;229:67–69. [PubMed: 3925552]

Del Negro CA, Morgado-Valle C, Feldman JL. Respiratory rhythm: An emergent network property? Neuron 2002;34:821–830. [PubMed: 12062027]

Del Negro CA, Morgado-Valle C, Hayes JA, Mackay DD, Pace RW, Crowder EA, Feldman JL. Sodium and calcium current-mediated pacemaker neurons and respiratory rhythm generation. J Neurosci 2005;25:446–453. [PubMed: 15647488]

DeMarse TB, Wagenaar DA, Blau AW, Potter SM. The Neurally Controlled Animat: Biological brains acting with simulated bodies. Auton Robots 2001;11:305–310.

Dugandzijanovakovic S, Shrager P. Survival, Development, and Electrical-Activity of Central-Nervous-System Myelinated Axons Exposed to Tumor-Necrosis-Factor In-Vitro. J Neurosci Res 1995;40:117–126. [PubMed: 7714919]

Feldman JL, Mitchell GS, Nattie EE. Breathing: rhythmicity, plasticity, chemosensitivity. Annu.Rev.Neurosci 2003;26:239–266. [PubMed: 12598679]

Filosa JA, Putnam RW. Multiple targets of chemosensitive signaling in locus coeruleus neurons: role of K^{+} and $Ca2^{+}$ channels. Am J Physiol Cell Physiol 2003;284:C145–C155. [PubMed: 12388081]

Fukuda Y, See WR, Honda Y. H^{+}-sensitivity and pattern of discharge of neurons in the chemosensitive areas of the ventral medulla oblongata of rats in vitro. Pflugers Arch 1980;388:53–61. [PubMed: 7192389]

Gerstein GL, Perkel DH. Mutual temporal relationships among neuronal spike trains. Statistical techniques for display and analysis. Biophys J 1972;12:453–473. [PubMed: 5030560]

NIH-PA Author Manuscript

NIH-PA Author Manuscript

NIH-PA Author Manuscript

Gerstein GL, Aertsen AM. Representation of cooperative firing activity among simultaneously recorded neurons. J Neurophysiol 1985;54:1513–1528. [PubMed: 4087046]

Gerstein GL. Cross-correlation measures of unresolved multi-neuron recordings. J Neurosci Methods 2000;100:41–51. [PubMed: 11040365]

Gustafsson B, Jankowska E. Direct and indirect activation of nerve cells by electrical pulses applied extracellularly. J Physiol 1976;258:33–61. [PubMed: 940071]

Guyenet PG, Stornetta RL, Bayliss DA, Mulkey DK. Retrotrapezoid nucleus: a litmus test for the identification of central chemoreceptors. Exp Physiol 2005;90:247–253. [PubMed: 15728136]

Guyenet PG, Mulkey DK, Stornetta RL, Bayliss DA. Regulation of ventral surface chemoreceptors by the central respiratory pattern generator. J Neurosci 2005;25:8938–8947. [PubMed: 16192384]

He DS, Burt JM. Mechanism and selectivity of the effects of halothane on gap junction channel function. Circ.Res 2000;86:E104–E109. [PubMed: 10850971]

Hebb, DO. The Organization of Behavior. New York: Wiley; 1949. The Organization of Behavior.

Horn CC, Friedman MI. Detection of single unit activity from the rat vagus using cluster analysis of principal components. J Neurosci Methods 2003;122:141–147. [PubMed: 12573473]

Huang RQ, Erlichman JS, Dean JB. Cell-cell coupling between CO_2-excited neurons in the dorsal medulla oblongata. Neurosci 1997;80:41–57.

Jiang C, Lipski J. Extensive monosynaptic inhibition of ventral respiratory group neurons by augmenting neurons in the Botzinger complex in the cat. Exp.Brain Res 1990;81:639–648. [PubMed: 2226695]

Jiang C, Xu H, Cui N, Wu J. An alternative approach to the identification of respiratory central chemoreceptors in the brainstem. Respir.Physiol 2001;129:141–157. [PubMed: 11738651]

Jiang C, Rojas A, Wang RP, Wang XR. CO_2 central chemosensitivity: why are there so many sensing molecules? Respir Physiol Neurobiol 2005;145:115–126. [PubMed: 15705527]

Kawaguchi H, Fukunishi K. Dendrite classification in rat hippocampal neurons according to signal propagation properties. Observation by multichannel optical recording in cultured neuronal networks. Exp.Brain Res 1998;122:378–392. [PubMed: 9827857]

Kawai A, Ballantyne D, Muckenhoff K, Scheid P. Chemosensitive medullary neurones in the brainstem-spinal cord preparation of the neonatal rat. J Physiol Lond 1996;492:277–292. [PubMed: 8730602]

Kawai A, Onimaru H, Homma I. Mechanisms of CO_2/H^+ chemoreception by respiratory rhythm generator neurons in the medulla from newborn rats in vitro. J Physiol 2006;572:525–537. [PubMed: 16469786]

LaneLadd SB, Pineda J, Boundy VA, Pfeuffer T, Krupinski J, Aghajanian GK, Nestler EJ. CREB (cAMP response element-binding protein) in the locus coeruleus: Biochemical, physiological, and behavioral evidence for a role in opiate dependence. J Neurosci 1997;17:7890–7901. [PubMed: 9315909]

Li Z, Morris KF, Baekey DM, Shannon R, Lindsey BG. Multimodal medullary neurons and correlational linkages of the respiratory network. J Neurophysiol 1999;82:188–201. [PubMed: 10400947]

Li A, Nattie E. Catecholamine neurones in rats modulate sleep, breathing, central chemoreception and breathing variability. J Physiol 2006;570:385–396. [PubMed: 16254009]

Lieske SP, Thoby-Brisson M, Telgkamp P, Ramirez JM. Reconfiguration of the neural network controlling multiple breathing patterns: eupnea, sighs and gasps. Nat.Neurosci 2000;3:600–607. [PubMed: 10816317]

Mao JZ, Li L, McManus M, Wu JP, Cui NR, Jiang C. Molecular determinants for activation of G-protein-coupled inward rectifier K^+ (GIRK) channels by extracellular acidosis. J Biol Chem 2002;277:46166–46171. [PubMed: 12361957]

Mulkey DK, Stornetta RL, Weston MC, Simmons JR, Parker A, Bayliss DA, Guyenet PG. Respiratory control by ventral surface chemoreceptor neurons in rats. Nat.Neurosci 2004;7:1360–1369. [PubMed: 15558061]

Nattie E. CO_2, brainstem chemoreceptors and breathing. Prog.Neurobiol 1999;59:299–331. [PubMed: 10501632]

Nattie EE, Gdovin M, Li AH. Retrotrapezoid Nucleus Glutamate Receptors - Control of CO_2-Sensitive Phrenic and Sympathetic Output. J Appl Physiol 1993;74:2958–2968. [PubMed: 8103513]

Neubauer JA, Gonsalves SF, Chou W, Geller HM, Edelman NH. Chemosensitivity of medullary neurons in explant tissue cultures. Neurosci 1991;45:701–708.

NIH-PA Author Manuscript

NIH-PA Author Manuscript

NIH-PA Author Manuscript

Nusbaum MC, Blitz DM, Swensen AM, Wood D, Marder E. The roles of co-transmission in neural network modulation. Trends Neurosci 2001;24:146–154. [PubMed: 11182454]

Okada Y, Chen Z, Jiang W, Kuwana S, Eldridge FL. Anatomical arrangement of hypercapnia-activated cells in the superficial ventral medulla of rats. J Appl Physiol 2002;93:427–439. [PubMed: 12133847]

Onimaru H, Arata A, Homma I. Firing properties of respiratory rhythm generating neurons in the absence of synaptic transmission in rat medulla in vitro. Exp Brain Res 1989;76:530–536. [PubMed: 2551710]

Oyamada Y, Ballantyne D, Muckenhoff K, Scheid P. Respiration-modulated membrane potential and chemosensitivity of locus coeruleus neurones in the in vitro brainstem-spinal cord of the neonatal rat. J Physiol Lond 1998;513:381–398. [PubMed: 9806990]

Palm G, Aertsen AM, Gerstein GL. On the significance of correlations among neuronal spike trains. Biol Cybern 1988;59:1–11. [PubMed: 3401513]

Perkel DH, Gerstein GL, Moore GP. Neuronal spike trains and stochastic point processes II. Simultaneous spike trains. Biophys J 1967;7(4):440.

Perkel, DH. Spike trains as carriers of information. In: Schmitt, FO., editor. The Neurosciences: A Second Study Program. Rockefeller University Press; 1970. p. 587-596.

Pilowsky P, Llewellyn-Smith IJ, Arnolda L, Lipski J, Minson J, Chalmers J. Are the ventrally projecting dendrites of respiratory neurons a neuroanatomical basis for the chemosensitivity of the ventral medulla oblongata? sleep 2006;16:S53–S55. [PubMed: 8178025]

Pineda J, Aghajanian GK. Carbon dioxide regulates the tonic activity of locus coeruleus neurons by modulating a proton- and polyamine-sensitive inward rectifier potassium current. Neurosci 1997;77:723–743.

Potter SM, DeMarse TB. A new approach to neural cell culture for long-term studies. J Neurosci Methods 2001;110:17–24. [PubMed: 11564520]

Putnam RW, Filosa JA, Ritucci NA. Cellular mechanisms involved in CO_2 and acid signaling in chemosensitive neurons. Am J Physiol Cell Physiol 2004;287:C1493–C1526. [PubMed: 15525685]

Ramirez JM, Tryba AK, Pena F. Pacemaker neurons and neuronal networks: an integrative view. Curr Opin Neurobiol 2004;14:665–674. [PubMed: 15582367]

Richerson GB, Getting PA. Preservation of integrative function in a perfused guinea pig brain. Brain Res 1990;517:7–18. [PubMed: 2376008]

Richerson GB. Serotonergic neurons as carbon dioxide sensors that maintain ph homeostasis. Nat.Rev.Neurosci 2004;5:449–461. [PubMed: 15152195]

Rigatto H, Fitzgerald SF, Willis MA, Yu C. In Search of the Real Respiratory Neurons - Culture of Medullary Fetal Cells Sensitive to CO_2 and Low Ph. Biol Neonate 1994;65:149–155. [PubMed: 8038275]

Rosenberg JR, Amjad AM, Breeze P, Brillinger DR, Halliday DM. The Fourier approach to the identification of functional coupling between neuronal spike trains. Prog Biophys Mol Biol 1989;53:1–31. [PubMed: 2682781]

Severson CA, Wang WG, Pieribone VA, Dohle CI, Richerson GB. Midbrain serotonergic neurons are central pH chemoreceptors. Nat.Neurosci 2003;6:1139–1140. [PubMed: 14517544]

Smith JC, Ellenberger HH, Ballanyi K, Richter DW, Feldman JL. Pre-Botzinger complex: a brainstem region that may generate respiratory rhythm in mammals. science 1991;254:726–729. [PubMed: 1683005]

Solomon IC, Halat TJ, El Maghrabi MR, O'Neal MH. Localization of connexin26 and connexin32 in putative CO_2-chemosensitive brainstem regions in rat. Respir Physiol 2001;129:101–121. [PubMed: 11738649]

Solomon IC, Dean JB. Gap junctions in CO_2-chemoreception and respiratory control. Respir Physiol Neurobiol 2002;131:155–173. [PubMed: 12126918]

Solomon IC. Connexin36 distribution in putative CO_2-chemosensitive brainstem regions in rat. Respir Physiol Neurobiol 2003;139:1–20. [PubMed: 14637306]

Solomon IC, Chon KH, Rodriguez MN. Blockade of brain stem gap junctions increases phrenic burst frequency and reduces phrenic burst synchronization in adult rat. J Neurophysiol 2003;89:135–149. [PubMed: 12522166]

NIH-PA Author Manuscript

NIH-PA Author Manuscript

NIH-PA Author Manuscript

Stunden CE, Filosa JA, Garcia AJ, Dean JB, Putnam RW. Development of in vivo ventilatory and single chemosensitive neuron responses to hypercapnia in rats. Respir Physiol 2001;127:135–155. [PubMed: 11504586]

Stunden CE, Garcia AJ, Filosa JA, Dean JB, Putnam RW. Correlation between the in vivo ventilatory and central chemosensitive neuron responses to hypercapnia in neonatal rats. FASEB J 2001;15:A151.

Su J, Jiang C. Multicellular recordings of cultured brainstem neurons in microelectrode arrays. Cell Tissue Res 2006;326:25–33. [PubMed: 16767404]

Su J, Yang L, Zhang XL, Rojas A, Shi Y, Jiang C. High CO_2 chemosensitivity versus wide sensing spectrum: A paradoxical problem and its solutions in cultured brainstem neurons. J Physiol 2007;578:831–841. [PubMed: 17124273]

Takakura AC, Moreira TS, Colombari E, West GH, Stornetta RL, Guyenet PG. Peripheral chemoreceptor inputs to retrotrapezoid nucleus (RTN) CO_2-sensitive neurons in rats. J Physiol 2006;572:503–523. [PubMed: 16455687]

Takakura ACT, Moreira TS, Colombari E, West GH, Stornetta RL, Guyenet PG. Peripheral chemoreceptor inputs to retrotrapezoid nucleus (RTN) CO_2-sensitive neurons in rats. J Physiol Lond 2006;572:503–523. [PubMed: 16455687]

Wagenaar DA, Madhavan R, Pine J, Potter SM. Controlling bursting in cortical cultures with closed-loop multi-electrode stimulation. J Neurosci 2005;25:680–688. [PubMed: 15659605]

Wagenaar DA, Madhavan R, Pine J, Potter SM. Controlling bursting in cortical cultures with closed-loop multi-electrode stimulation. J Neurosci 2005;25:680–688. [PubMed: 15659605]

Wang WA, Richerson GB. Chemosensitivity of non-respiratory rat CNS neurons in tissue culture. Brain Res 2000;860:119–129. [PubMed: 10727630]

Wang WG, Pizzonia JH, Richerson GB. Chemosensitivity of rat medullary raphe neurones in primary tissue culture. J Physiol Lond 1998;511:433–450. [PubMed: 9706021]

Wemmie JA, Chen J, Askwith CC, Hruska-Hageman AM, Price MP, Nolan BC, Yoder PG, Lamani E, Hoshi T, Freeman JH Jr, Welsh MJ. The acid-activated ion channel ASIC contributes to synaptic plasticity, learning, and memory. Neuron 2002;34:463–477. [PubMed: 11988176]

Young KC, Peracchia C. Opposite Cx32 and Cx26 voltage-gating response to CO_2 reflects opposite voltage-gating polarity. J Membr Biol 2004;202:161–170. [PubMed: 15798904]

NIH-PA Author Manuscript
NIH-PA Author Manuscript
NIH-PA Author Manuscript

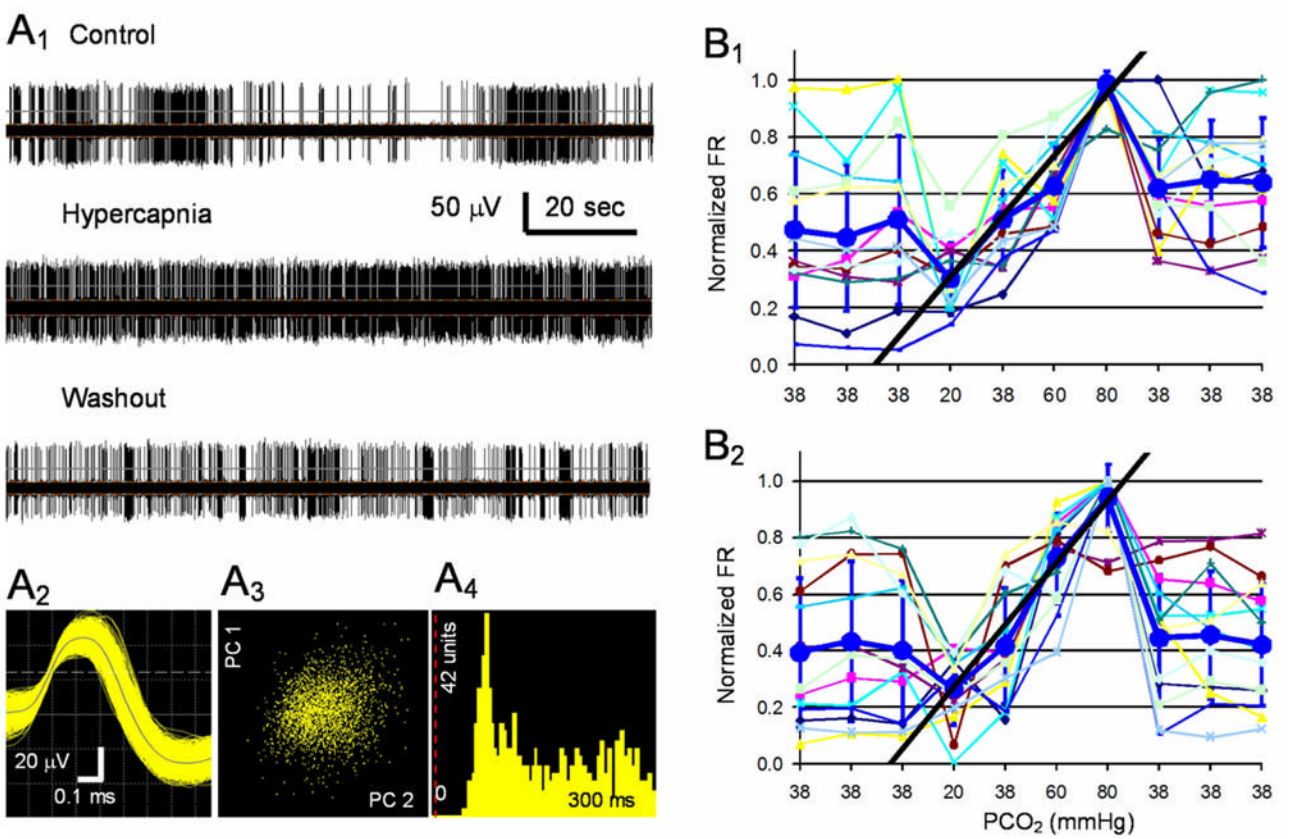

Fig. 1.

CO_2 chemosensitivity of single unit recorded in the MEA. **A_1.** A single unit was recorded from one channel of an MEA dish (upper). The unit was stimulated reversibly with an exposure to 10% CO_2 (middle), and its firing activity returned to the baseline level after washout (lower). **A_2.** The digitized action potentials show a duration >1ms. Note that the longer negative wave was not shown. **A_3.** The PCA shows that all spikes detected are clustered in the X-Y axis system, where the X axis is PC2 (i.e., the waveform projection onto the first principal component) and Y axis is PC1 (i.e., the waveform projection onto the 2nd principal component). **A_4.** The interspike histogram indicates single-unit recording because of the lack of action potentials in the initial 20ms. **B_1**. Thirteen units were recorded in another MEA dish. The firing rate (FR) of these units was modulated by CO_2 in a concentration-dependent manner. A linear response in the FR was seen in PCO_2 20 – 80 torr. Note that each symbol indicates a unit, and the average of all units is shown as large circles and thicker line (means ± S.D.). The FR response can be described with a linear equation as shown with the straight line, and the slope value or the C value is 0.011. **B_2**. The response was reproducible as seen with repetitive exposure in a 24-hr interval with the C value 0.011.

NIH-PA Author Manuscript

NIH-PA Author Manuscript

NIH-PA Author Manuscript

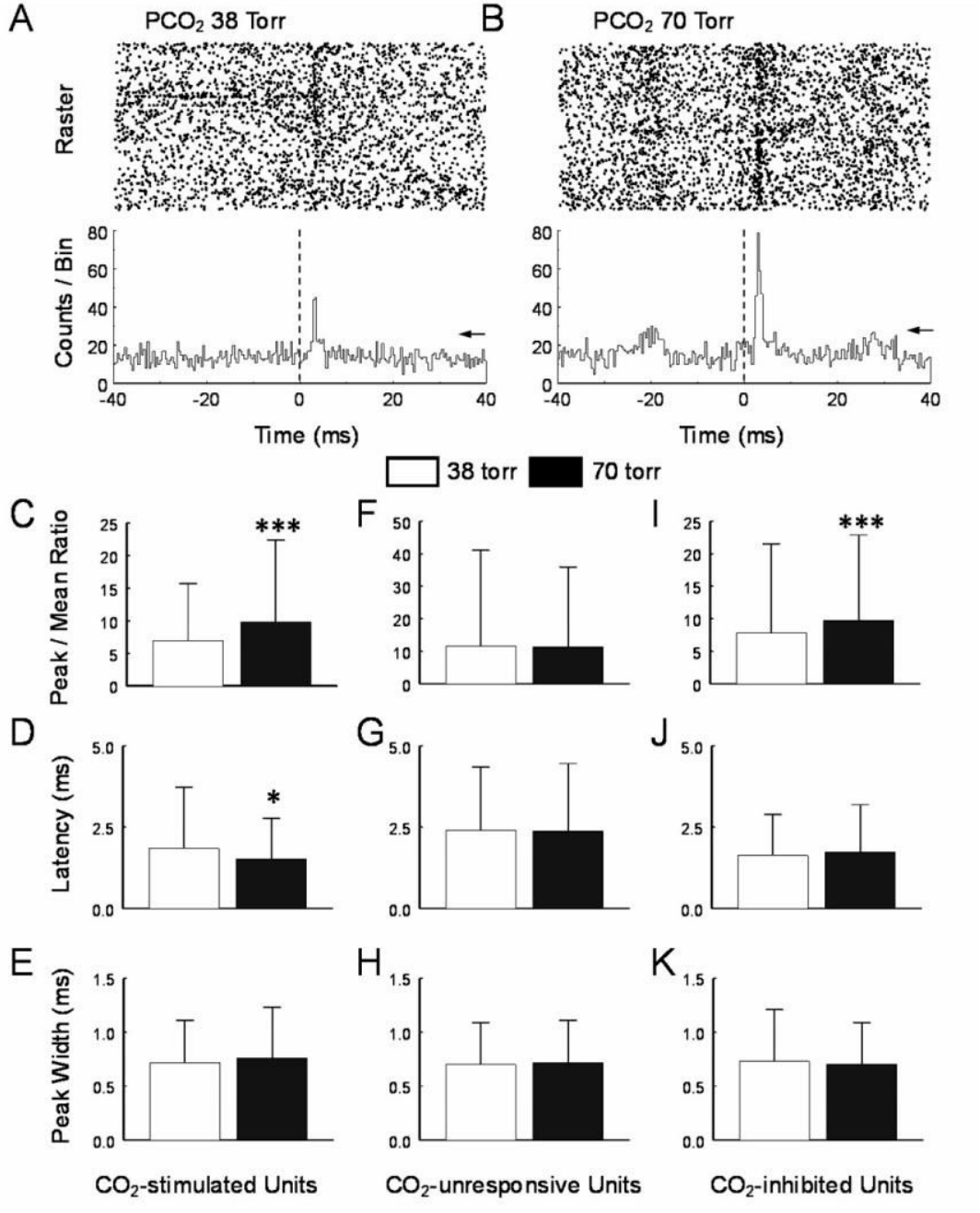

Fig. 2.

The peri-central peak. **A.** A peri-event histogram (PEH) was built between two CO_2-stimulated units. In the raster display (upper), action potentials of the target unit show a higher occurrence about 2 ms after spiking of the reference unit at baseline PCO_2 (38 torr). Average of the spikes of the target unit shows a clear pericentral peak in the PEH (lower). The peak is significantly greater than the 99.9% confidence level (arrow). **B.** During hypercapnic exposure (PCO_2 70 torr), the peak increased markedly, while the background counts also rose to a less degree. In CO_2-stimulated units, the average peak-mean ratio was significantly higher during hypercapnia than in baseline (**C**), the peak latency was reduced (**D**), and the peak width did not show significant changes (**E**). Similar analysis was done in CO_2-unresponsive units, but none of the

peak-mean ratio (**F**), peak latency (**G**), and peak width (**H**) changed significantly. **I–K**, In CO_2 inhibited units, only the peak-mean ration increased significantly. *, P<0.05, **; P<0.01; ***, P<0.001. Data are represented as mean ± S.D.

NIH-PA Author Manuscript
NIH-PA Author Manuscript
NIH-PA Author Manuscript

NIH-PA Author Manuscript
NIH-PA Author Manuscript
NIH-PA Author Manuscript

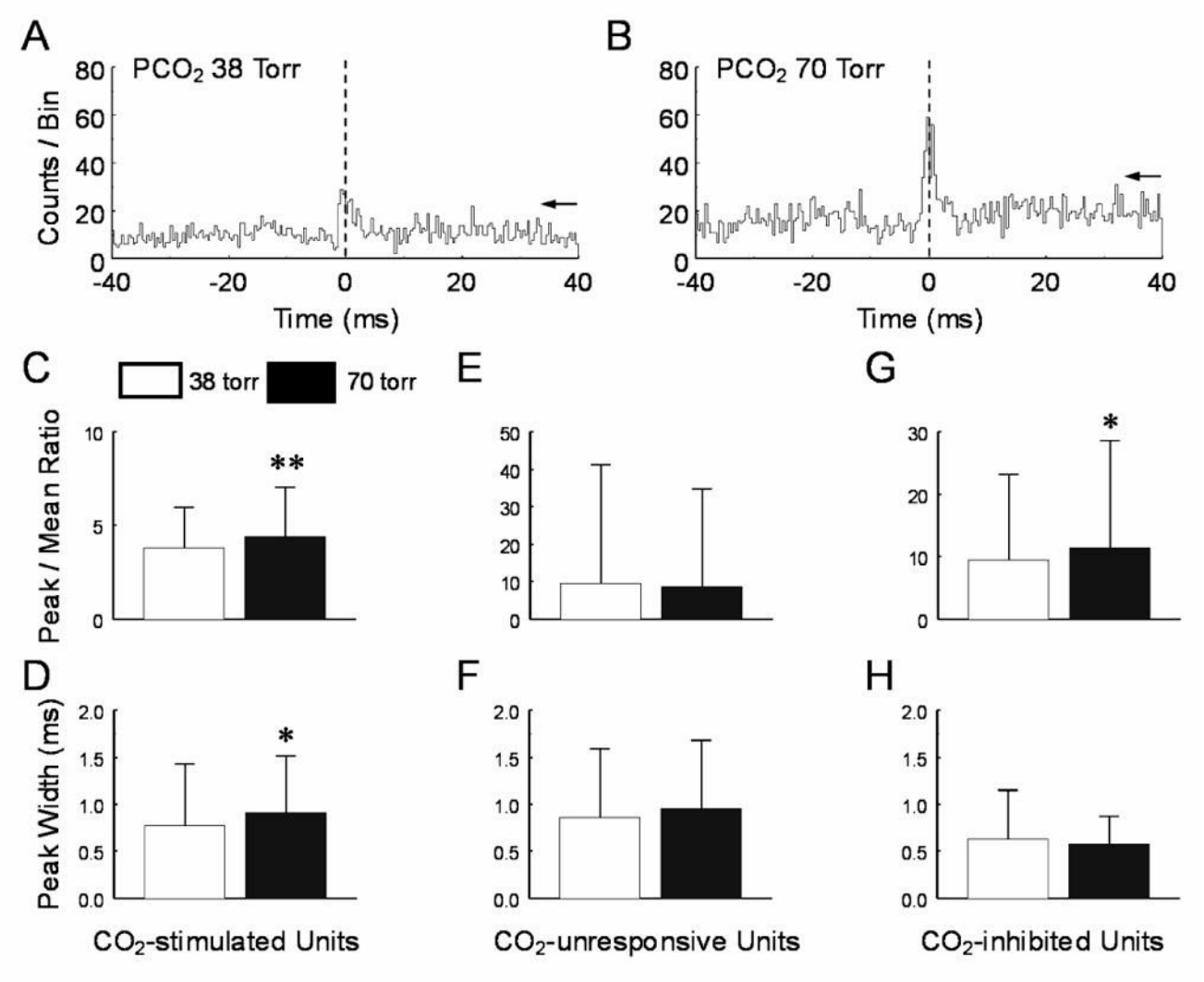

Fig. 3.

The central peak. **A, B.** Peri-event histograms showed that the amplitude of the central peak between two CO_2-stimulated units was higher during hypercapnia. **C, D.** Significant increases of the peak-mean ratio and peak width were observed in CO_2-stimulated units. Hypercapnia did not alter these values in CO_2-unresponsive (**E, F**) and CO_2-inhibited units (**G, H**). *, $P<0.05$; **, $P<0.01$. Data are represented as mean ± S.D.

NIH-PA Author Manuscript

NIH-PA Author Manuscript

NIH-PA Author Manuscript

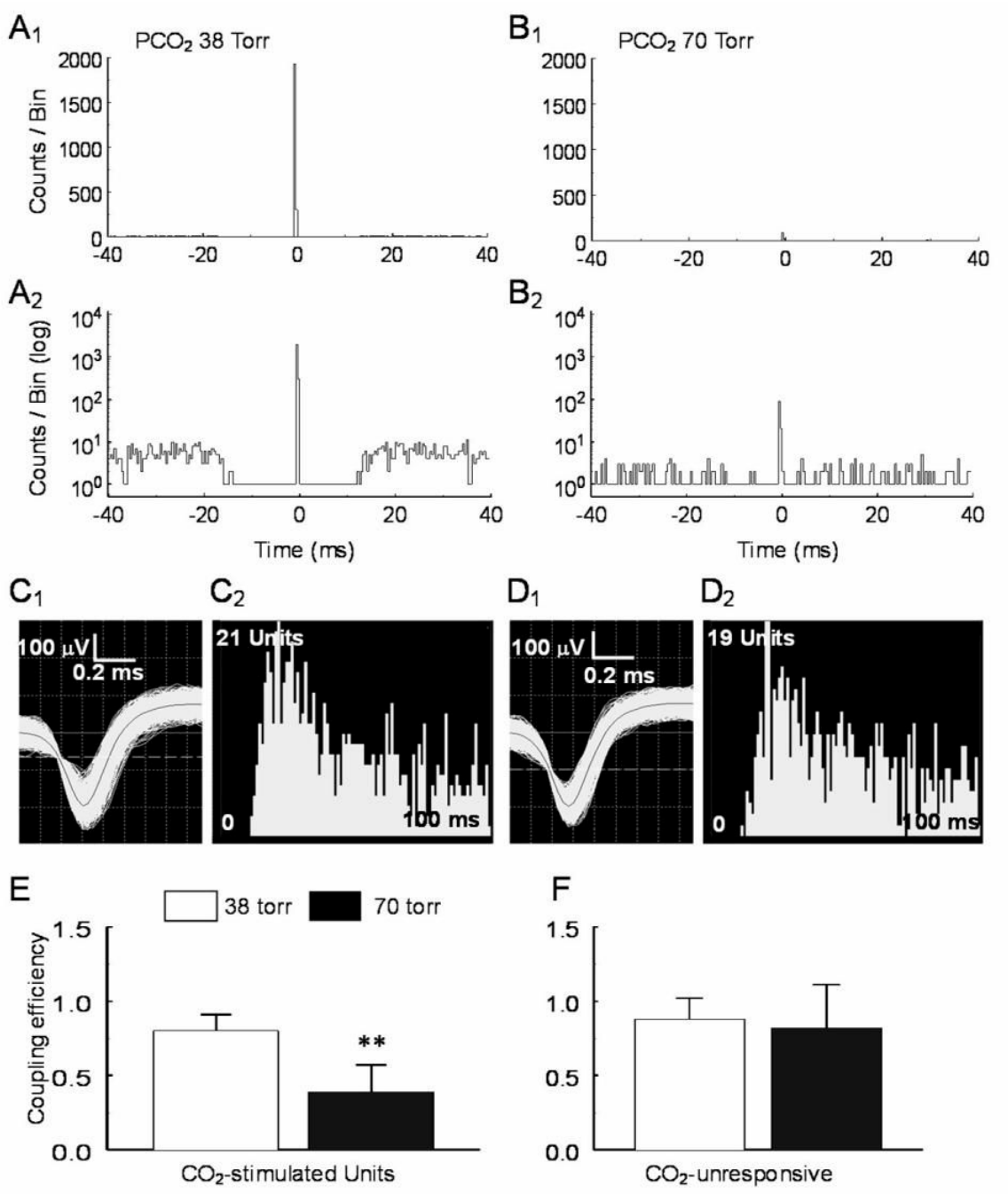

Fig. 4.

Suppression of electrical coupling during hypercapnia. **A.** A sharp central peak was seen in a pair of CO_2-stimulated units. The spike trains of these units occurred almost always simultaneously with the background counts barely seen in regular scale (**A_1**). Seen in log scale (**A_2**), the background counts were not symmetric (coupling efficiency = 0.99). **B_1, B_2.** The coupling between these units was greatly diminished during high CO_2 exposure (coupling efficiency = 0.10). **C, D.** The spike morphology and interspike histograms show single unit recordings with action potential duration > 1ms (**C_1, D_1**) for both units. **E, F.** Statistical analysis show that the electrical coupling is suppressed in CO_2-stimulated units (P=0.006, n=4) but not in CO_2-unresponsive units (P=0.21, n=12). Data are represented as mean ± S.D.

NIH-PA Author Manuscript

NIH-PA Author Manuscript

NIH-PA Author Manuscript

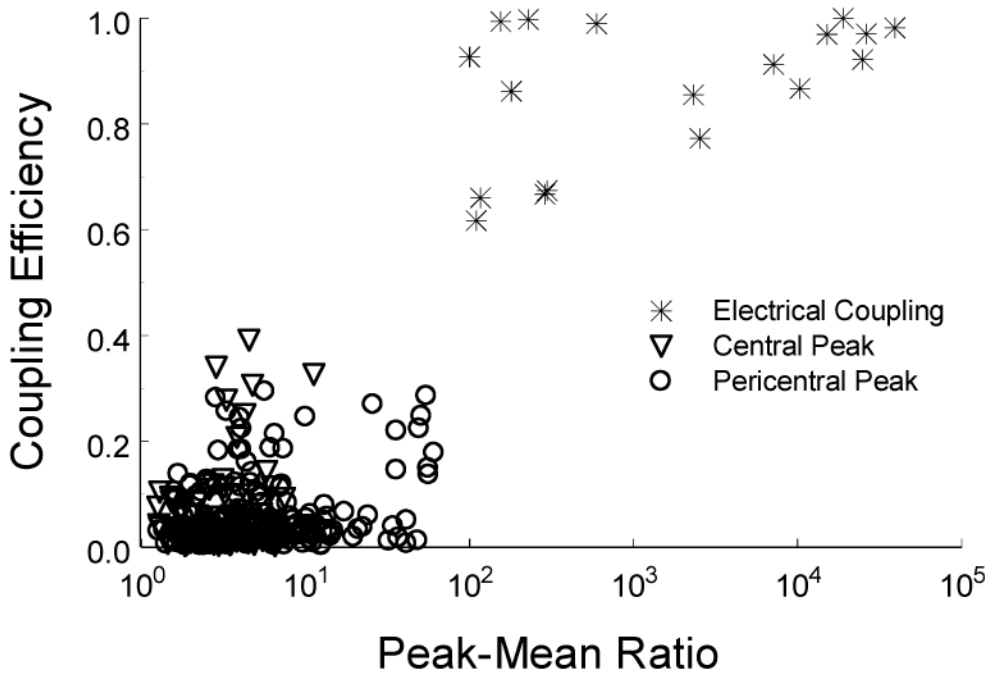

Fig. 5.

Plot of central peak and electrical coupling using coupling efficiency vs. peak-mean ratio. The pericentral peak and central peak go into one cluster whereas electrical coupling forms another clear cluster.

NIH-PA Author Manuscript

NIH-PA Author Manuscript

NIH-PA Author Manuscript

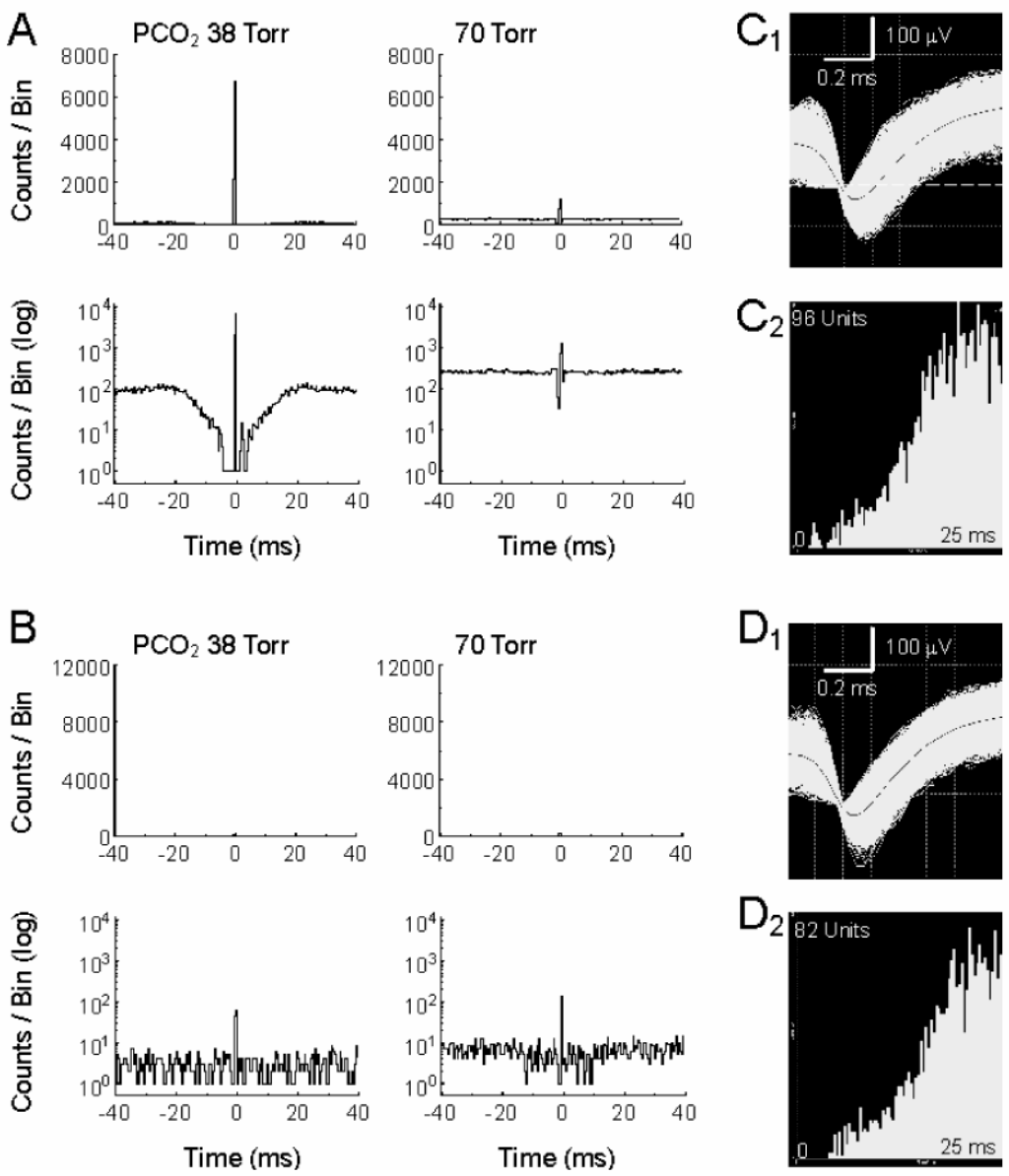

Fig. 6.

Sensitivity of the electrical coupling to halothane. **A.** Electrical coupling was seen in a pair of CO_2-stimulated units (coupling efficiency = 0.91). The electrical coupling was strongly and reversibly inhibited with hypercapnia (coupling efficiency = 0.17). **B.** The electrical coupling was also strongly inhibited by 2mM halothane (coupling efficiency = 0.18). In the presence of halothane, hypercapnia failed to inhibit the electrical coupling (coupling efficiency = 0.21). **C, D.** Action potential morphology and interspike internal analyses indicate that these units are single and recorded from soma.

NIH-PA Author Manuscript
NIH-PA Author Manuscript
NIH-PA Author Manuscript

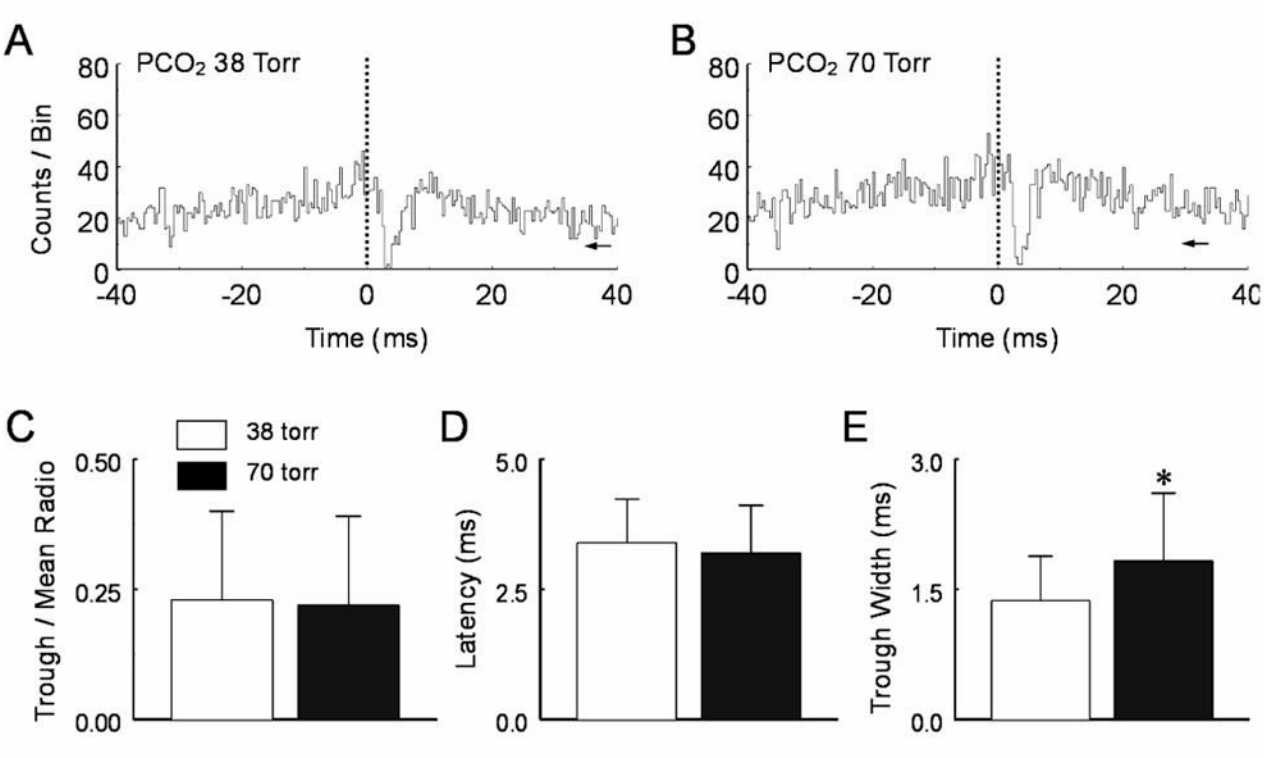

Fig. 7.

Hypercapnic effects on pericentral troughs. **A.** A narrow pericentral trough was seen in the PEH with the reference unit CO_2-stimulated and target unit CO_2-inhibited. **B.** Hypercapnia had very little effect on the pericentral trough. **C, D.** Statistical analysis indicates that none of the trough/mean ratio and trough latency is affected by hypercapnia. **E.** The trough width at half magnitude is enhanced at PCO_2 70 torr ($P<0.05$, $n=5$). Data are represented as mean ± S.D.

NIH-PA Author Manuscript
NIH-PA Author Manuscript
NIH-PA Author Manuscript

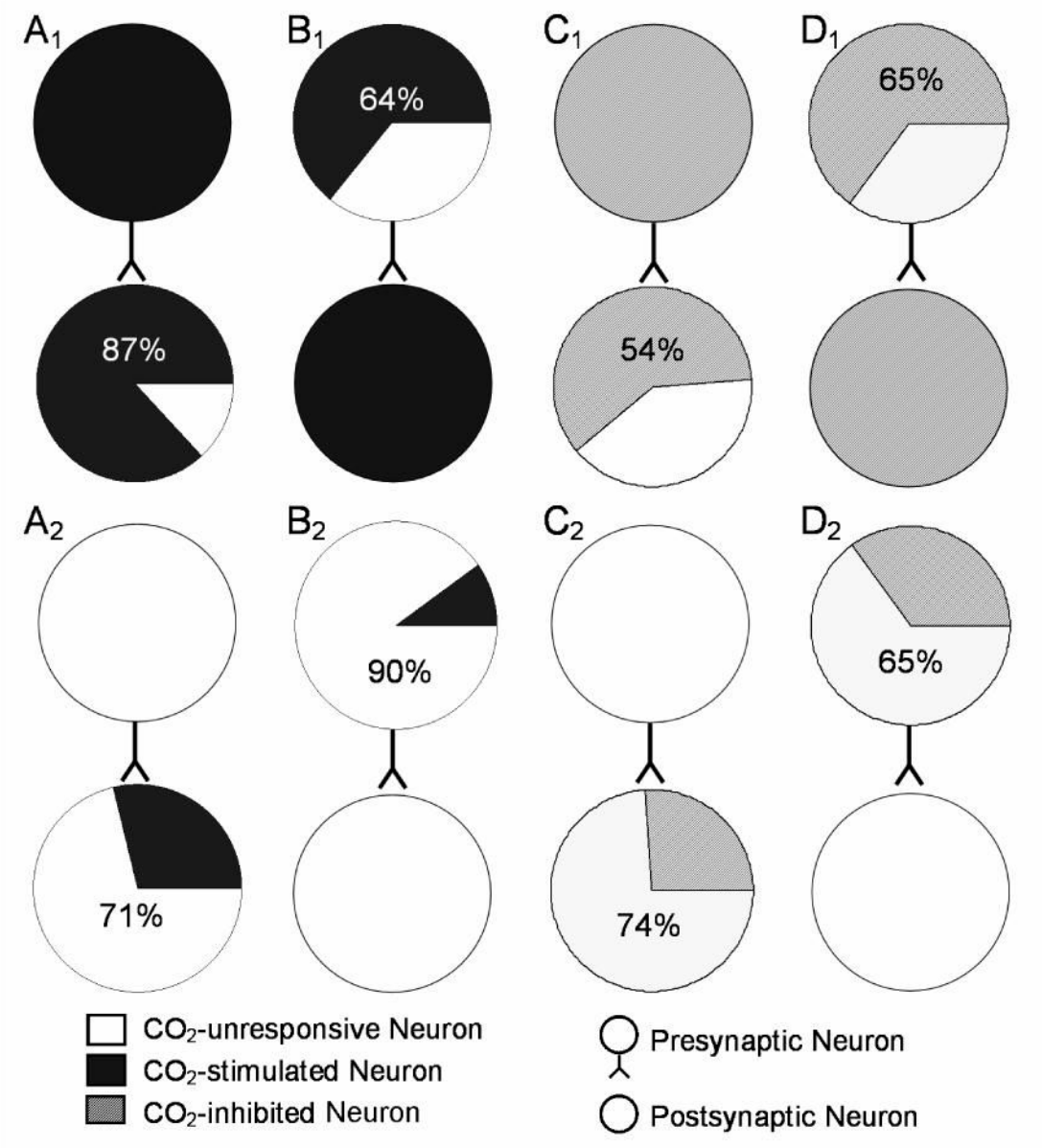

Fig. 8.

Connection preference of cultured brainstem neurons. **A.** Concerning reference units, 87% CO_2-stimulated units projected to another CO_2-stimulated units (**A_1**), while only 29% CO_2-unresponsive units projected to CO_2-stimulated units (**A_2**). **B.** With respect to target units, 64% CO_2-stimulated units received synaptic input from another CO_2-stimulated units (**B_1**). Only 10% CO_2-unresponsive received such synaptic input (**B_2**). **C**. For the reference units, 54% CO_2-inhibited neurons projected to another CO_2-inhibited units (**C_1**), whereas only 26% CO_2-unresponsive units projected to the CO_2-inhibited units (**C_2**). **D**. From the target units, 65% CO_2-inhibited neuron received synaptic input from another CO_2-inhibited units (**D_1**), but only 46% CO_2-unresponsive units received synaptic inputs from another CO_2-inhibited units (**D_2**).

NIH-PA Author Manuscript

NIH-PA Author Manuscript

NIH-PA Author Manuscript

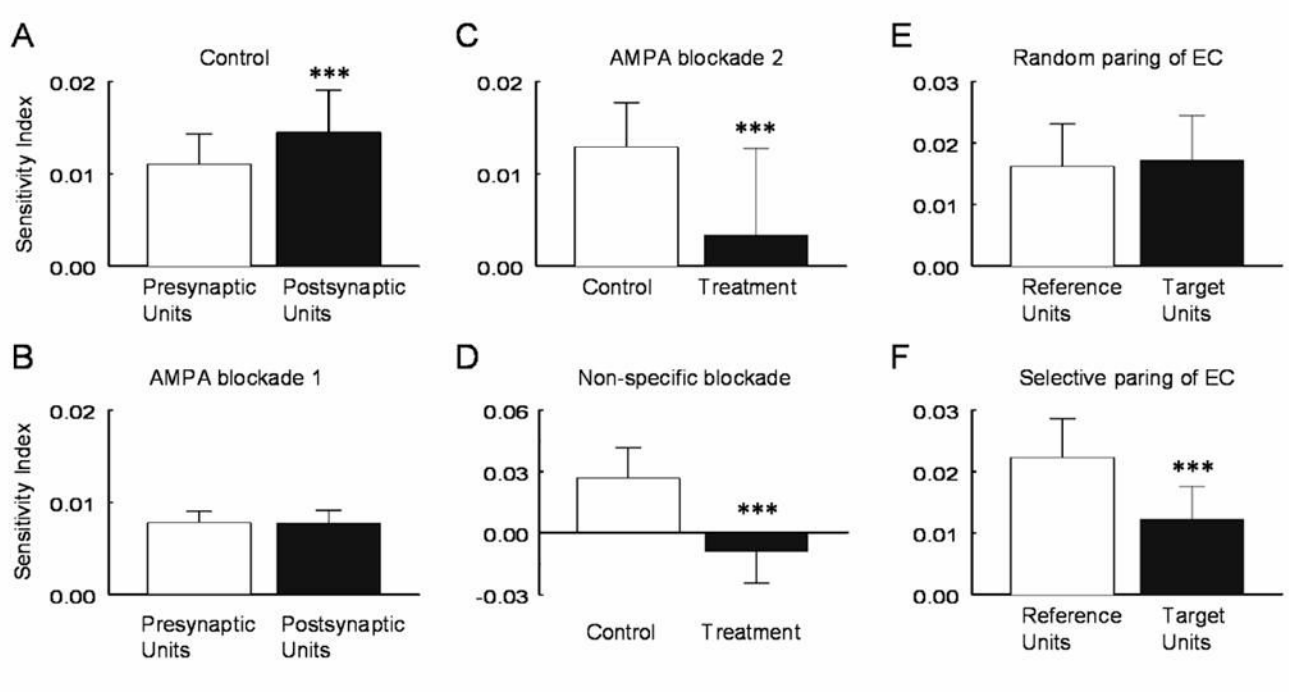

Fig. 9.

Enhancement of CO_2 sensitivity by synapse transmission. **A**. With intact synaptic transmission, the post-synaptic neurons had a C value significantly higher than the presynaptic units (P=9.0E-06, n=61). **B.** Such a difference was abolished by a blockade of excitatory synaptic transmission with 10μM CNQX (P=0.45, n=13). C. In the presence of 10μM CNQX, some units lost the CO_2 chemosensitivity almost completely (P=7.0E-05, n=20). **D**. Similar effect was seen with a non-specific blockade of synaptic transmission using low Ca^{2+} (<1 μM) and high concentrations of Mg^{2+} (2 mM) (P=3.3E-06, n=13). **E.** Both reference and target units showed identical CO_2 sensitivity when they were grouped randomly (P=0.45, n=4). **F.** However, one of the units in each pair showed much higher CO_2 sensitivity than the other when they were pooled together (P=0.0004, n=4). Data are represented as mean ± S.D.

NIH-PA Author Manuscript NIH-PA Author Manuscript NIH-PA Author Manuscript

Table 1

Summary of Network Properties of Cultured Brainstem Neurons

	PCO_2 38 torr		70 torr				
	mean	**S.D.**	**mean**	**S.D.**	**# U**	**# D**	**P**
CO_2-stimulated units							
Peak-mean ratio (total)	5.62	7.10	7.55	10.09	106	4	<0.001
Peak-mean ratio (pericentral)	6.92	8.82	9.80	12.60	62	4	<0.001
Pericentral peak latency (ms)	1.85	1.89	1.52	1.26	62	4	0.01
Pericentral peak width (ms)	0.72	0.39	0.76	0.47	62	4	0.19
Peak-mean ratio (central)	3.78	2.19	4.39	2.65	44	4	0.003
Central peak width (ms)	0.77	0.66	0.91	0.60	44	4	0.03
Electrical coupling efficiency	0.80	0.11	0.39	0.18	5	3	0.006
Trough/mean ratio	0.23	0.17	0.22	0.17	6	3	0.33
Trough latency (ms)	3.40	0.83	3.20	0.91	6	3	0.15
Trough width (ms)	1.37	0.51	1.83	0.78	6	3	0.03
CO_2-unresponsive units							
Peak-mean ratio (total)	11.14	29.88	10.69	24.97	221	4	0.45
Peak-mean ratio (pericentral)	11.61	29.42	11.31	24.63	168	4	0.61
Pericentral peak latency (ms)	2.41	1.94	2.39	2.07	168	4	0.94
Pericentral peak width (ms)	0.70	0.39	0.72	0.39	168	4	0.31
Peak-mean ratio (central)	9.66	31.52	8.72	25.99	53	4	0.29
Central peak width (ms)	0.86	0.73	0.95	0.73	53	4	0.13
Electrical coupling efficiency	0.88	0.14	0.82	0.29	13	10	0.21
CO_2-inhibited units							
Peak-mean ratio (total)	8.30	13.75	10.22	13.86	127	7	<0.001
Peak-mean ratio (pericentral)	7.87	13.69	9.77	13.12	93	7	<0.001
Pericentral peak latency (ms)	1.63	1.25	1.74	1.45	93	7	0.19
Pericentral peak width (ms)	0.73	0.48	0.70	0.39	93	7	0.09
Peak-mean ratio (central)	9.46	13.76	11.44	17.08	34	7	0.02
Central peak width (ms)	0.63	0.52	0.58	0.29	34	7	0.18

Differences between the PCO_2 levels were examined using Student t test with P value shown in the last column. Abbreviations: # D, number of dishes; # U, number of units; P, probability; S.D., standard deviation.